 CMES, vol.91, no.6, pp.463-484, 2013

A Fast Regularized Boundary Integral Method for Practical Acoustic Problems

Z.Y. Qian, Z.D. Han[1], and S.N. Atluri[1,2]

Abstract: To predict the sound field in an acoustic problem, the well-known non-uniqueness problem has to be solved. In a departure from the common approaches used in the prior literature, the weak-form of the Helmholtz differential equation, in conjunction with vector test-functions, is utilized as the basis, in order to directly derive non-hyper-singular boundary integral equations for the velocity potential ϕ, as well as its gradients q. Both ϕ-BIE and q-BIE are fully regularized to achieve weak singularities at the boundary [i.e., containing singularities of $O(r^{-1})$]. Collocation-based boundary-element numerical approaches [denoted as BEM-R-ϕ-BIE, and BEM-R-q-BIE] are implemented to solve these. To overcome the drawback of fully populated system matrices in BEM, the fast multipole method is applied, and denoted here as FMM-BEM. The computational costs of FMM-BEM are at the scale of $O(2nN)$, which make it much faster than the matrix based operation, and suitable for large practical problems of acoustics.

Keywords: Boundary integral equations, Fast multilevel multipole algorithm

1 Introduction

It is well known that the solutions of the conventional boundary integral equations are nonunique at the fictitious eigenfrequencies for exterior acoustic or elastic wave problems in the frequency domain. The fictitious eigenfrequencies have no physical meaning for the exterior problems, and are the manifestations of the drawback of the mathematical formulation of the conventional boundary element method. To circumvent this, hypersingular boundary integral equations (HBIEs), which are the derivatives of the conventional boundary integral equations, have become a useful alternative approach. Liu and Chen (1999) and Burton and Miller (1971) linearly combine the surface Helmholtz integral equation for the potential, and the integral

[1] Center for Aerospace Research & Education, University of California, Irvine, CA 92612, USA
[2] Distinguished Visiting Professor of Multi-Disciplinary Engineering and Computer Science, King Abdul Aziz University, Saudi Arabia

equation for the normal derivative of potential at the surface (HBIEs), to circumvent the problem of nonuniqueness at characteristic frequencies. Their method is very effective, and is labeled as CHIE (Composite Helmholtz Integral Equation), or CONDOR (Composite Outward Normal Derivative Overlap Relation) by Reut [Reut (1985)]. However, the smoothness requirement, which implies that the derivatives of the density function must be Holder continuous, is a serious theoretical issue associated with the HBIE formulation [Liu and Chen (1999)]. Therefore, only boundary elements with C^1 continuity near each node, such as the Overhauser and Hermite elements, can be applied in the implementation of HBIEs [Liu and Rizzo (1992)]. This requirement hinders the applications of HBIEs, because of the complexity of C^1 elements. Another key issue for hypersingular boundary integral equations, is the application of regularization techniques, which are commonly employed to improve the approach by reducing the problem to the one involving $O(r^{-1})$ singular integrals near the point of singularity. Chien, Rajiyah, and Atluri (1990) employed some known identities of the fundamental solution from the associated interior Laplace problem, to regularize the hypersingular integrals. This concept has been applied by many successive researchers: The regularized normal derivative equation in Wu, Seybert, and Wan (1991) is sought to be convergent in the Cauchy principal value sense, rather than in the finite-part sense, and the computation of tangential derivatives is required everywhere on the boundary. Yan, Hung, and Zheng (2003) employed a discretized operator matrix for improving the intensive computation of double surface integrals, by replacing the evaluation of double surface integral with the evaluation of two discretized operator matrices. In general, most of *the regularization techniques* published so far in literature for evaluating the hyper-singular integrals in the acoustic BIEs, arise from certain identities associated with the fundamental solution to the Laplace equations.

However, in the present paper, without directly differentiating the derivatives of the conventional boundary integral equation for the potential, which will result in the hyper-singular integrals, novel non-hyper-singular boundary integral equations are derived directly, for the gradients of the velocity potential. The acoustic potential gradients are related to the sound velocity in their physical meaning. The basic idea of using the gradients of the fundamental solution to the Helmholtz differential equation, as *vector test-functions* to write the weak-form of the original Helmholtz differential equation, and thereby directly derive a *non-hyper-singular boundary integral equations for velocity potential gradients*, has its origins in [Okada, Rajiyah, and Atluri (1988a), Okada, Rajiyah, and Atluri (1988b), Okada, Rajiyah, and Atluri (1989), Okada, Rajiyah, and Atluri (1990), and Okada and Atluri (1994)], who use the displacement and velocity gradients to directly establish the displacement and displacement gradient boundary integral equations in elastic/plastic solid problems,

as well as traction boundary integral equations [Han and Atluri (2003a), and Han and Atluri (2003b)], which are very simple to be implemented numerically. The current method can be shown to be fundamentally different from the regularized normal derivative equation by Wu *et al*. [Wu, Seybert, and Wan (1991)], who used the tangential derivatives to reduce the singularity.

The boundary integral equations for the potential [labeled here as ϕ-BIE] and its gradient [labeled here as q-BIE] are further regularized to *only weakly singular* [$O(r^{-1})$] types, which are labeled here as R-ϕ-BIE, R-q-BIE, respectively. This is achieved *by using certain basic identities of the fundamental solution of the Helmholtz differential equation for potential*. These basic identities, in their most general form, are also newly derived in this paper. These basic identities are derived from the most general scalar and vector weak-forms of the Helmholtz differential equation for potential, *governing the fundamental solution itself*. The boundary element methods [BEM] derived by simply collocating the R-ϕ-BIE, and R-q-BIE, are referred to as the BEM-R-ϕ-BIE, and BEM-R-$q-$BIE, respectively.

To speed up the numerical calculation of the boundary integral equations and overcome the drawback of fully populated system matrices in BEM further, the Fast Multipole Method (FMM) is introduced. FMM is a technique for calculating sums of the form:

$$f(x_i) = \sum_{j=1}^{N} K(x_i, y_j)\sigma_j \qquad i = 1, \ldots, N \tag{1}$$

in $O(N)$ operations with a user-defined error ε. It is firstly proposed by Greengard and Rokhlin [Greengard and Rokhlin (1987)] for the kernel, $K(x,y) = 1/r, \quad (r = |x-y|)$, and the technique is based on Legendre polynomials and spherical harmonics, which was later extended to the oscillatory kernel e^{ikr}/r. Both these approaches require approximations of $K(x,y)$ for $|x-y|$ sufficiently large that are typically obtained using known analytical expansions. Fong developed a "black-box" FMM or "kernel independent" FMM [Fong and Darve (2009)], which is to increase the calculation efficiency for the boundary integral equations. This black-box FMM is quite different from many fast multipole methods which depend on analytical expansions of the far field behavior of K, for $|x-y|$ large, and require a small pre-computation time even for very large systems, and uses the minimal number of coefficients to represent the far field, for a given L^2 tolerance error in the approximation [Nishimura (2002)].

The black-box FMM extends the fast multipole method to general kernels, which are demonstrated possible by kernel-independent FMMs, as shown in [Martinsson

and Rokhlin (2007); Ying, Biros, and Zorin (2004)]. Fewer methods exist which allow building a fast $O(N)$ method using only numerical values of K, that is without requiring approximations based on analytical expansions. These techniques are often based on wavelet decompositions [Dahmen, Harbrecht, and Schneider (2006); Alpert, Beylkin, Coifman, and Rokhlin (1993)], singular value decompositions [Gimbutas, Greengard, and Minion (2001); Gimbutas and Rokhlin (2003)], or other schemes [Martinsson and Rokhlin (2007); Cheng, Gimbutas, Martinsson, and Rokhlin (2005)]. [Ethridge and Greengard (2001); Dutt and Rokhlin (1993); Edelman, McCorquodale, and Toledo (1999)] used interpolation techniques (e.g., Chebyshev polynomials) in various ways as part of constructing fast methods. The reference [Dutt, Gu, and Rokhlin (1996)] discusses a similar idea, with some differences, including the fact that the multipole and local expansions are treated differently, whereas our scheme is more "symmetrical" and treats them in a similar way. In addition, [Dutt, Gu, and Rokhlin (1996)] focuses on a 1 dimensional FMM with the kernel $1/r$, which is required by their fast algorithm for interpolation, differentiation and integration.

In present paper, a Chebyshev interpolation based FMM method combined with GMRES iterative solver is utilized to implement the BEM-R-ϕ-BIE, and BEM-R-q-BIE. Compared to other FMM methods published in literatures, the present FMM-BEM is kernel independent through using Chebyshev interpolation, which is more flexible for the programming. Moreover, by implementing the regularized BIE, the algorithm becomes more stable and suitable for complex geometry, which is superior to those FMM based traditional BEM methods in literatures. And the computation cost is at the scale of $O(N)$, which is suitable for large practical problems.

2 The regularized boundary integral equations in acoustics

The Helmholtz differential equation governing the acoustic velocity potential ϕ for time-harmonic $e^{i\omega t}$ waves, can be written as:

$$\nabla^2\phi + k^2\phi = 0 \tag{2}$$

where i is the imaginary unit, ω is the angular frequency of the acoustic wave, and $k = \omega/c$ is the wave number. At any field point ξ, the velocity potential of Eq. 1, due to a point sound source at $\mathbf{x}$, is well known as the free-space Green's function $\phi^*(\mathbf{x},\xi)$. Therefore, the so-called fundamental solution of the Helmholtz equation is governed by the wave equation,

$$\phi^*_{,ii}(\mathbf{x},\xi)+k^2\phi^*(\mathbf{x},\xi)+\delta(\mathbf{x},\xi)=0 \tag{3}$$

2.1 Regularized boundary integral equations for the velocity potential ϕ-BIE

By using $\bar{\phi}$ as the test function to enforce the Helmholtz equation, Eq. 2 in terms of the trial function ϕ, in a weak-sense, the weak form of Helmholtz equation can be written as,

$$\int_\Omega \left(\nabla^2\phi+k^2\phi\right)\bar{\phi}d\Omega=0 \tag{4}$$

A "symmetric weak-form" is obtained by applying the divergence theorem once in Eq. 4,

$$\int_{\partial\Omega} n_i\phi_{,i}\bar{\phi}dS-\int_\Omega \phi_{,i}\bar{\phi}_{,i}d\Omega+\int_\Omega k^2\phi\bar{\phi}d\Omega=0 \tag{5}$$

where, both the trial function ϕ, as well as the test functions $\bar{\phi}$ are only required to be first-order differentiable. By applying the divergence theorem twice in Eq. 4, we obtain the "unsymmetric weak-form",

$$\int_{\partial\Omega} n_i\phi_{,i}\bar{\phi}dS-\int_{\partial\Omega} n_i\phi\bar{\phi}_{,i}dS+\int_\Omega \phi\left(\bar{\phi}_{,ii}+k^2\bar{\phi}\right)d\Omega=0 \tag{6}$$

Now, the test functions $\bar{\phi}$ are required to be second-order differentiable, while ϕ is not required to be differentiable [Han and Atluri (2003a)] in Ω.

By using the fundamental solution $\phi^*(\mathbf{x},\xi)$ as the test function $\bar{\phi}$ in Eq. 6, and with the property from Eq. 3, we obtain the integral equation for ϕ:

$$\phi(\mathbf{x})=\int_{\partial\Omega} q(\xi)\,\phi^*(\mathbf{x},\xi)\,dS-\int_{\partial\Omega}\phi(\xi)\,\Theta^*(\mathbf{x},\xi)\,dS \quad \mathbf{x}\in\Omega \tag{7}$$

where, by definition,

$$q(\xi)=\frac{\partial\phi(\xi)}{\partial n_\xi}=n_k(\xi)\,\phi_{,k}(\xi) \quad \xi\in\partial\Omega$$

and the kernel function $\Theta^*(\mathbf{x},\xi)$ is defined as,

$$\Theta^*(\mathbf{x},\xi)=\frac{\partial\phi^*(\mathbf{x},\xi)}{\partial n_\xi}=n_k(\xi)\,\phi^*_{,k}(\mathbf{x},\xi) \quad \xi\in\partial\Omega$$

Eq. 7 is the conventional BIE for ϕ, which is widely used in literature, and is hereafter referred to as the ϕ-BIE. One can also use Green's second identity directly to obtain Eq. 7.

The nonuniqueness of the Helmholtz integral equation, Eq. 7, is well known; it possesses nontrivial solutions at some characteristic frequencies [Chien, Rajiyah, and Atluri (1990)]. Many researchers have investigated and expended substantial efforts in solving this problem of nonuniqueness.

Eq. 7 can be implemented numerically without any difficulty, if it is restricted only for boundary points, ie., $\mathbf{x} \in \partial\Omega$, because $n_k(\xi)\phi^*_{,k}(\mathbf{x},\xi)$ contains only the weak singularity $[\mathrm{O}(r^{-1})]$. Most researchers have implemented the ϕ-BIE based on this equation and solved the boundary problems. On the other hand, when one consider a domain point which is approaching the boundary, one may encounter the higher order singularity $[\mathrm{O}(r^{-2})]$ with Eq. 7. The ϕ-BIE can be regularized further as shown in [Qian, Han, Ufimtsev, and Atluri (2004)], for a point $\mathbf{x}$ on the boundary $\partial\Omega$, as:

$$\int_{\partial\Omega} q(\xi)\,\phi^*(\mathbf{x},\xi)\,dS - \int_{\partial\Omega} [\phi(\xi)-\phi(\mathbf{x})]\,\Theta^*(\mathbf{x},\xi)\,dS = \int_{\partial\Omega}^{CPV} \Theta^*(\mathbf{x},\xi)\,\phi(\mathbf{x})\,dS + \frac{1}{2}\phi(\mathbf{x}) \quad \mathbf{x}\in\partial\Omega \tag{8}$$

in which CPV denotes a Cauchy Principal Value integral, $\phi(\xi)-\phi(\mathbf{x})$ becomes $\mathrm{O}(r)$ when $\xi \to \mathbf{x}$, and at the same time Eq. 8 becomes weakly-singular $[\mathrm{O}(r^{-1})]$. A reference node on the boundary may be used for a point close to the boundary, for regularization purpose. [Han and Atluri (2003a)]. Therefore, one can evaluate all the integrals in Eq. 8 numerically, for both the boundary points and the points close to the boundary. *We refer to Eq. 8 as the regularized ϕ-BIE or "R-ϕ-BIE", which involves singularities of order* $\mathrm{O}(r^{-1})$ *only.*

If $\partial\Omega$ has corners, ϕ may be expected to have a variation of $r^{+\lambda}$ $(\lambda<1)$ near the corners. In such cases, $\phi(\xi)-\phi(\mathbf{x})$ may become $O(r^{\lambda-1})$ when $\xi\to\mathbf{x}$, and thus, in a theoretical sense, Eq. 8 is no longer weakly singular. However, in a numerical solution of R-φ-BIE Eq. 8 directly, through a collocation process, to derive a ϕ *Boundary Element Method (BEM-R-ϕ-BIE)*, we envision using only C^0 polynomial interpolations of ϕ and q. Thus, in the numerical implementation of the BEM-R-ϕ-BIE by a collocation process, we encounter only weakly singular integrals. By using C^0 elements and employing an adaptive boundary-element refinement strategy near corners at the boundary, one may extract the value of $(\lambda<1)$ in the asymptotic solution for ϕnear such a corner [Qian, Han, Ufimtsev, and Atluri

(2004)].

2.2 Regularized boundary integral equations for q-BIE

We can write *a vector weak-form* [as opposed to a scalar weak-form] of the governing equation Eq. 4 by using the vector test function $\bar{\phi}_{,k}$, as in [Okada, Rajiyah, and Atluri (1989a, 1989b)]:

$$\int_{\Omega} \left(\phi_{,ii} + k^2\phi\right) \bar{\phi}_{,k} d\Omega = 0 \quad \text{for k=1,2,3} \tag{9}$$

After applying the divergence theorem three times in Eq. 8, and by using the gradients of the fundamental solution, viz., $\phi^*_{,k}(\mathbf{x},\xi)$, as the test functions, and using the identity from Eq. 3, we obtain

$$\begin{aligned} -\phi_{,k}(\mathbf{x}) = \int_{\partial\Omega} q(\xi)\,\phi^*_{,k}(\mathbf{x},\xi)\,dS + \int_{\partial\Omega} D_t\phi(\xi)\,e_{ikt}\,\phi^*_{,i}(\mathbf{x},\xi)\,dS \\ + \int_{\partial\Omega} k^2 n_k(\xi)\,\phi(\xi)\,\phi^*(\mathbf{x},\xi)\,dS \end{aligned} \tag{10}$$

we have used the definition of the surface tangential operator as

$$D_t = n_r e_{rst} \frac{\partial}{\partial \xi_s}$$

in which e_{rst} is the permutation symbol.

We refer to Eq. 10, hereafter, as the presently proposed non-hyper-singular q-BIE. The ϕ-BIE [Eq. 7], and q-BIE [Eq. 10], *are derived independently of each other*. The most interesting feature of the "directly derived" integral equations Eq. 10, for $\phi_{,k}(\mathbf{x})$, *is that they are non-hyper-singular*, viz, *the highest order singularity in the kernels appearing in Eq.* (9) *is only* $O\left(r^{-2}\right)$ *in a 3D problem.*

By using the basic properties of the fundamental solutions, and contracting with $n_k(\mathbf{x})$ on both sides, we can obtain the fully regularized form of Eq. 10 as,

$$\begin{aligned} -\frac{1}{2}q(\mathbf{x}) = \int_{\partial\Omega} \left[q(\xi) - n_i(\xi)\,\psi_i(\mathbf{x})\right] \hat{\Theta}^*(\mathbf{x},\xi)\,dS \\ + \int_{\partial\Omega} k^2 n_k(\mathbf{x})\,n_k(\xi)\,\phi(\xi)\,\phi^*(\mathbf{x},\xi)\,dS \\ + \int_{\partial\Omega} \left[D_t\phi(\xi) - (D_t\phi)(\mathbf{x})\right] n_k(\mathbf{x})\,e_{ikt}\,\phi^*_{,i}(\mathbf{x},\xi)\,dS \\ + \int_{\partial\Omega}^{CPV} \Theta^*(\mathbf{x},\xi)\,q(\mathbf{x})\,dS \end{aligned} \tag{11}$$

where the kernel function $\hat{\Theta}^*(\mathbf{x},\xi)$ is defined as,

$$\hat{\Theta}^*(\mathbf{x},\xi) = -\frac{\partial\phi^*(\mathbf{x},\xi)}{\partial n_x} = n_k(\mathbf{x})\frac{\partial\phi^*(\mathbf{x},\xi)}{\partial\xi_k} \quad \xi \in \partial\Omega$$

and $\psi(\mathbf{x})$ is defined in terms of $\phi_{,i}(\mathbf{x})$ on the boundary, as,

$$\begin{cases} \psi_3(\mathbf{x}) = q(\mathbf{x}) \\ \psi_1(\mathbf{x}) = t_i(\mathbf{x})\phi_{,i}(\mathbf{x}) \\ \psi_2(\mathbf{x}) = s_i(\mathbf{x})\phi_{,i}(\mathbf{x}) \end{cases} \tag{12}$$

We label Eq. 11 as the regularized q-BIE, or "R-q-BIE". Suppose $\partial\Omega$ is smooth; then $[q(\xi) - n_i(\xi)\psi_i(\mathbf{x})]$ and $[D_t\phi(\xi) - (D_t\phi)(\mathbf{x})]$ become $O(r)$ when $\xi \to \mathbf{x}$, and Eq. 11 becomes weakly singular $[O(r^{-1})]$ on a 3D problem. Thus, one can evaluate all the integrals in Eq. 11 numerically, and applicable to any point $\mathbf{x}$on the boundary $\partial\Omega$. On the other hand, if $\partial\Omega$ has corners, $[q(\xi) - n_i(\xi)\psi_i(\mathbf{x})]$ and $[D_t\phi(\xi) - (D_t\phi)(\mathbf{x})]$ become $O(r^{\lambda-1})$ when $\xi \to \mathbf{x}$, and thus, in a theoretical sense, Eq. 11 is no longer weakly singular. However, in a numerical implementation of the R-$q-$BIE, viz. Eq. 11, directly, *through a collocation process, to derive a q Boundary Element Method (BEM-R-q-BIE)*, we envision using only C^0 polynomial interpolations of ϕ and q. Thus, in the numerical implementation of the BEM-$q-$BIE by a collocation of Eq. 11, we encounter only weakly singular integrals.

3 The fast multilevel multipole algorithm with Chebyshev interpolation

In the numerical implementation of the boundary integral equations, it can be actually considered as the interaction of every combination of a load point with a field point, as expressed in Eq. 1, the kernel in which we can describe with an interpolation method, as follows:

$$K(x,y) \approx \sum_l \sum_m K(x_l,y_m) w_l(x) w_m(y) \tag{13}$$

where $w_l(x)$ are the interpolating functions. This is the so-called low-rank approximation, and can be used for any interpolation scheme. The advantage of this type of approach is that it requires minimal pre-computing. In addition, the only input required is the ability to evaluate K at various points, and no kernel-dependent analytical expansion is required.

3.1 The fast multilevel multipole algorithm

The multipole algorithm sets up a clustering and sums up the contribution of all sources in the center C_A of a cluster. The interaction between the source point and

the field point can be split up into three parts [Brunner, Junge, and Gaul (2009)]: neighbor, far-field signature, and near-field signature. The far-field signature measures the effect from the far-field clusters to the source, and the near-field signature measures the effect from the local clusters. All the transformations can be implemented b three operators: M2M (moment to moment), M2L (moment to local), L2L (local to local). The multipole expansion is valid only for well-separated load and field points, and one has to split up the clusters into a near- and far-field. The near-field is represented by a sparse matrix, which has to be evaluated by classical BEM. All other clusters are in the far-field, and form the so-called interaction list.

To implement the summation with optimal efficiency, a hierarchic multilevel cluster tree is used. It is set up by consecutive quartering such that a mother cluster is divided into four son clusters (quadtree in 2D, octree in 3D) on the next level. The procedure starts with the root cluster, which contains all elements of the model. The division is stopped if a specified number of elements per cluster are reached. These final clusters, which do not have any sons, are called leaf clusters. Two clusters are near neighbors if they are on the same refinement level and share at least one vertex. From this definition, a cluster is a near neighbor of itself. Two clusters are well-separated if they are on the same refinement level and not near neighbors. One cluster is an interaction cluster of cluster I, if it is the child of the near neighbors of cluster I's parent, and is well-separated from cluster I.

If the kernel contains discontinuities in its domain, e.g., the Laplacian kernel $1/|x-y|$, the low-rank representation is not applicable. In order for the low-rank approximation to accurately represent the kernel, the field and source points need to be well-separated, i.e., the two intervals are non-overlapping. Hence it can be thought of as a far-field approximation of the kernel $K(x,y)$. Local interactions involving field points and sources in non-well-separated intervals can also be computed with the far-field approximation by subdividing the intervals. On this refined scale, interactions between well-separated field points and sources can be treated. Applying this refinement recursively, a fast multilevel multipole (FMM) method can be constructed by combining this multilevel scheme with the FMM tree structure.

Let the root level of the tree (level 0) be the computational cluster containing all field points and sources. The algorithm for an R-level 1-D FMM is as follows:

1. Compute the near neighbor part by traditional BEM.
2. Evaluate the far-field signature for every leaf cluster through translation operator M2M.
3. Translate the far-field signature to all interaction cluster by means of the translation operators M2L and sum it up as the near-field signature N(s) there.

4. Shift the far-field signature to the mother cluster and repeat step 3 until the interaction list is empty by means of the translation operator L2L. And go to the opposite direction and shift the near-field signature to the son clusters until the leaf clusters are reached.

5. Sum everything up.

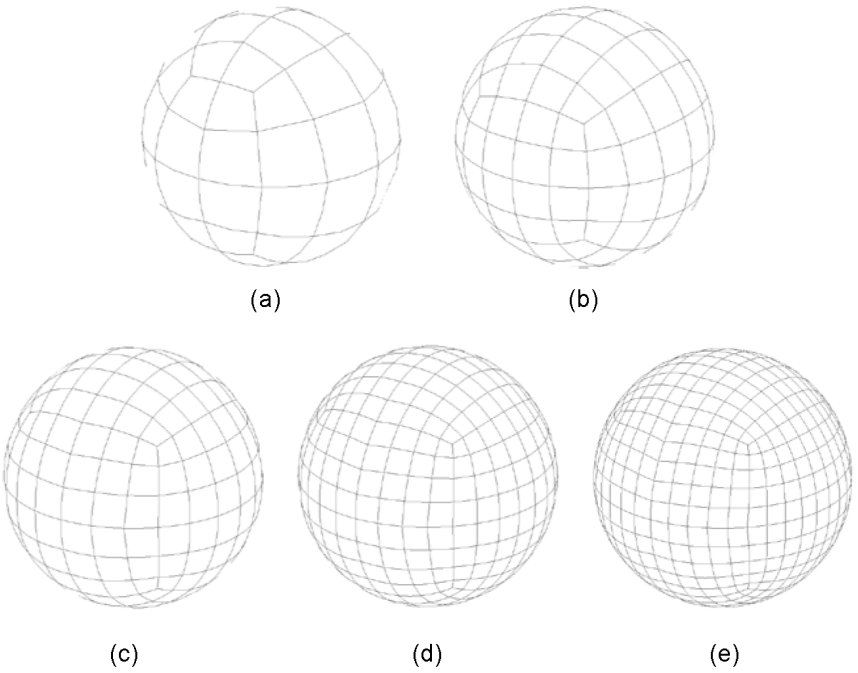

Figure 1: Surface discretization with quadrilateral elements (a) 194 nodes by 64 elements; (b) 386 Nodes by 128 Elements model; (c) 650 Nodes by 216 Elements; (d) 1154 Nodes by 384 Elements; (e) 1802 Nodes by 600 Elements

3.2 Chebyshev Polynomials as interpolation basis

One can construct a low-rank approximation of the kernel $K(x,y)$ by introducing an interpolation scheme. At first, let's consider a function $g(x)$ on the closed interval $[-1,1]$. An n-point interpolant that approximates $g(x)$ can be expressed as

$$p_{n-1}(x) = \sum_{l=1}^{n} g(x_l) w_l(x) \tag{14}$$

where x_l are the n interpolation nodes and $w_l(x)$ is the interpolating function corresponding to the node x_l. If the functions $w_l(x)$ are the Lagrange polynomials, then $p_{n-1}(x)$ is a $(n-1)$-degree polynomial approximation of $g(x)$. The above equation can be used to approximate the kernel $K(x,y)$ by first fixing the variable y and treating $K(x,y)$ as a function of x:

$$K(x,y) \approx \sum_{l=1}^{n} K(x_l, y) w_l(x) \tag{15}$$

The Chebyshev polynomials are the best to serve as the interpolation basis along with their roots as the interpolation nodes, for constructing a low-rank approximation in the fast multipole method, although any interpolation scheme can be used. Let's discuss some properties of the Chebyshev polynomials.

The first-kind Chebyshev polynomial of degree n, denoted by $T_n(x)$, is defined by the relation

$$T_n(x) = \cos(n\theta), \quad with\ x = \cos\theta \tag{16}$$

The domain of $T_n(x)$ is the closed interval $[-1,1]$. $T_n(x)$ has n roots located at

$$\bar{x}_m = \cos\theta_m = \cos\left(\frac{(2m-1)\pi}{2n}\right), \quad m = 1,\ldots,n \tag{17}$$

The set of roots $\{\bar{x}_m\}$ is commonly referred to as the Chebyshev nodes.

Using the Chebyshev nodes of $T_n(x)$ as the interpolation nodes, the polynomial $p_{n-1}(x)$ as an approximats to the function $g(x)$ can be expressed as a sum of Chebyshev polynomials

$$p_{n-1}(x) = \sum_{l=1}^{n} g(\bar{x}_l) S_n(\bar{x}_l, x) \tag{18}$$

where

$$S_n(x,y) = \frac{1}{n} + \frac{2}{n} \sum_{k=1}^{n-1} T_k(x) T_k(y) \tag{19}$$

Identifying $S_n(\bar{x}_l, x)$ as the interpolating function for the node $\bar{x}_l$, it follows from the previous equation that a low-rank approximation of the kernel $K(x,y)$ using Chebyshev polynomials is given by

$$K(x,y) \approx \sum_{l=1}^{n}\sum_{m=1}^{n} K(\bar{x}_l, \bar{y}_m) S_n(\bar{x}_l, x) S_n(\bar{y}_m, y) \tag{20}$$

Substituting this expression into Eq. 1 and changing the order of summation we have

$$\begin{aligned} f(x_i) &= \sum_{j=1}^{N} K(x_i - y_j)\sigma_j \\ &\approx \sum_{j=1}^{N}\left[\sum_{l=1}^{n}\sum_{m=1}^{n} K(\bar{x}_l, \bar{y}_m) S_n(\bar{x}_l, x_i) S_n(\bar{y}_m, y_j)\right]\sigma_j \\ &= \sum_{l=1}^{n} S_n(\bar{x}_l, x_i) \sum_{m=1}^{n} K(\bar{x}_l, \bar{y}_m) \sum_{j=1}^{N} \sigma_j S_n(\bar{y}_m, y_j) \end{aligned} \tag{21}$$

From this decomposition, a fast summation method using Chebyshev interpolation can be constructed. The computational cost of the three summations in the above equation are $O(nN)$, $O(n^2)$, and $O(nN)$ respectively. Hence for $n \ll N$ the algorithm scales like $O(2nN)$.

This fast summation method can also be extended to higher dimensions by taking a tensor product of the interpolating functions S_n, one for each dimension. For a 3-D kernel $K(\mathbf{x},\mathbf{y})$, where $\mathbf{x} = (x_1, x_2, x_3)$ and $\mathbf{y} = (y_1, y_2, y_3)$. The low-rank approximation of the kernel $K(\mathbf{x},\mathbf{y})$ using Chebyshev polynomials can be expressed as

$$K(\mathbf{x},\mathbf{y}) \approx \sum_{l=1}^{n}\sum_{m=1}^{n} K(\bar{x}_l, \bar{y}_m) R_n(\bar{x}_l, \mathbf{x}) R_n(\bar{y}_m, \mathbf{y}) \tag{22}$$

where

$$R_n(\mathbf{x},\mathbf{y}) = S_n(x_1, y_1) S_n(x_2, y_2) S_n(x_3, y_3) \tag{23}$$

and $\bar{x}_l = (\bar{x}_{l_1}, \bar{x}_{l_2}, \bar{x}_{l_3})$ and $\bar{y}_l = (\bar{y}_{m_1}, \bar{y}_{m_2}, \bar{y}_{m_3})$ are 3-vectors of Chebyshev nodes. [Fong and Darve (2009)]

4 Numerical results

In the implementation process, the BEM-R-ϕ-BIE and BEM-R-q-BIE are combined as in Eq. 24, and the coefficient β is chosen to be a small complex number.

$$\begin{aligned}
&\int_{\partial\Omega} q(\xi)\,\phi^*(\mathbf{x},\xi)\,dS - \int_{\partial\Omega}^{CPV} \Theta^*(\mathbf{x},\xi)\,\phi(\mathbf{x})\,dS \\
&\quad -\frac{1}{2}\phi(\mathbf{x}) - \int_{\partial\Omega} [\phi(\xi)-\phi(\mathbf{x})]\,\Theta^*(\mathbf{x},\xi)\,dS \\
&+\beta\{\frac{1}{2}q(\mathbf{x}) + \int_{\partial\Omega} [q(\xi)-n_i(\xi)\,\psi_i(\mathbf{x})]\,\hat{\Theta}^*(\mathbf{x},\xi)\,dS \\
&\quad + \int_{\partial\Omega} k^2 n_k(\mathbf{x})\,n_k(\xi)\,\phi(\xi)\,\phi^*(\mathbf{x},\xi)\,dS \\
&+ \int_{\partial\Omega} [D_t\phi(\xi) - (D_t\phi)(\mathbf{x})]\,n_k(\mathbf{x})\,e_{ikt}\,\phi^*_{,i}(\mathbf{x},\xi)\,dS \\
&\quad + \int_{\partial\Omega}^{CPV} \Theta^*(\mathbf{x},\xi)\,q(\mathbf{x})\,dS\} = 0
\end{aligned} \tag{24}$$

In order to check the accuracy and efficiency of the proposed method, two different representative acoustic problems are considered: (1) the pulsating sphere problem; and (2) acoustic scattering from a rigid UAV. The numerical codes are implemented with MATLAB, and running on Elitebook 8560w Laptop with 4G DDR3 SDRAM memory and 2nd generation Intel Core^{TM} i7 and i5 mobile processors.

4.1 Pulsating sphere

The field radiated from a pulsating sphere into the infinite homogeneous medium is chosen as an example for the exterior problem. The analytical solution for the acoustic pressure for a sphere of radius a, pulsating with uniform radial velocity v_a, is given by [Chien, Rajiyah, and Atluri (1990)]

$$\frac{p(r)}{z_0 v_a} = \frac{a}{r}\frac{ika}{1+ika}e^{-ik(r-a)} \tag{25}$$

where z_0 is the characteristic impedance, $p(r)$ is the acoustic pressure at distance r, and k is the wave number. For the purpose of comparison, BEM-R-[ϕ&q]-BIE and FMM-BEM, the whole sphere is considered for 64, 128, 216, 384, and 600 element model, as shown in Fig. 1. The models are discretized by using 8-node isoparametric quadrilateral elements. The evaluation of all integrals of kernels is performed by using 3x3 standard Gaussian quadrature.

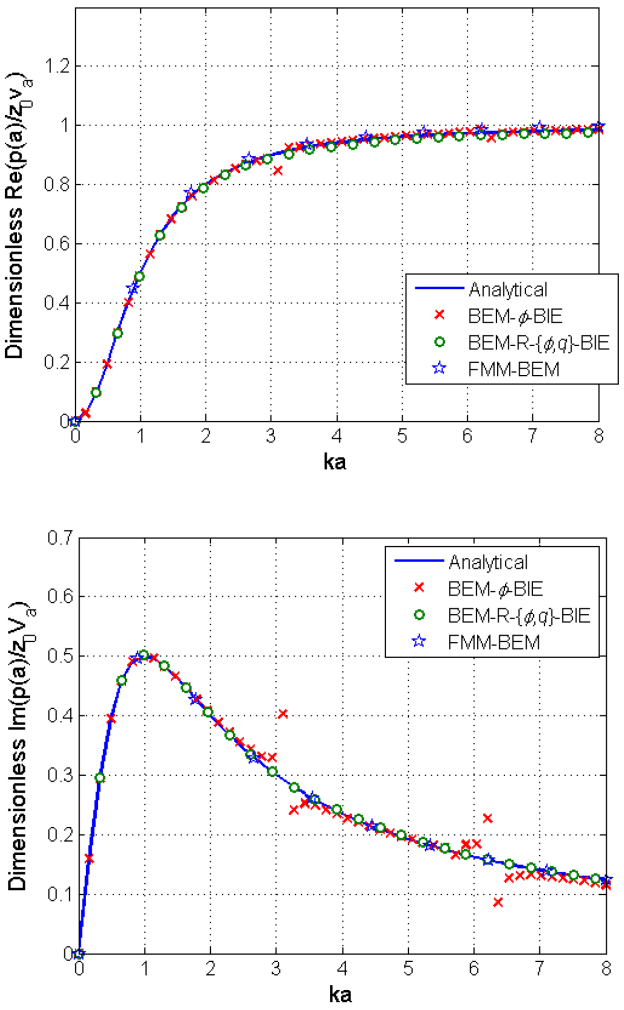

Figure 2: Dimensionless surface acoustic pressure of a pulsating (64 elements): (a) real part; (b) imaginary part

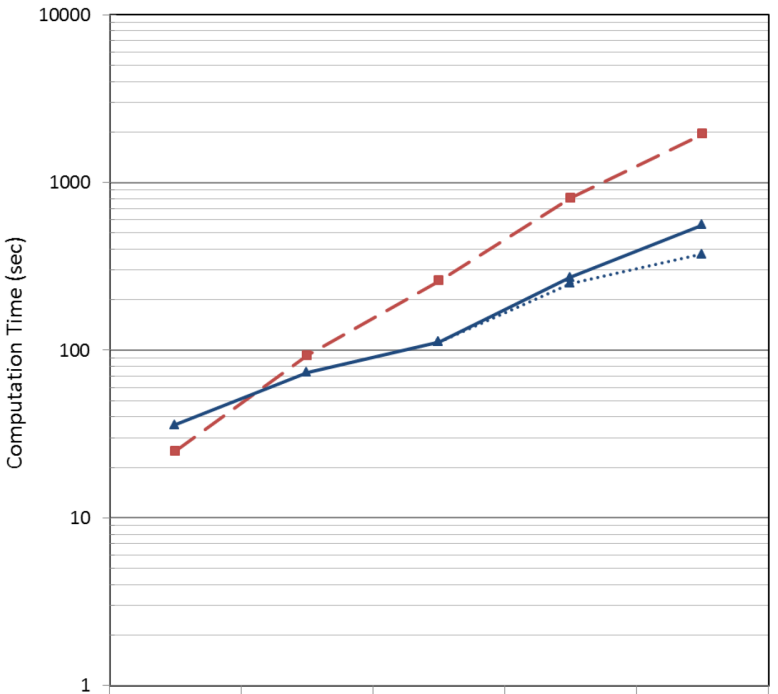

	194	386	650	1154	1802
BEM	25	93	259	808	1947
FMM_BIE	36	74	112	273	561
increase level			112	251	374

Figure 3: Comparison of computation time

In Fig. 2, the real and imaginary parts of dimensionless surface acoustic pressures are plotted with respect to the reduced frequency ka for 64 elements. The present results are seen to converge to the analytical solution. It is obvious that the conventional BIE method fails to provide unique solutions near $k = \pi, 2\pi \cdots$, which is also demonstrated in many earlier works, such as [Yan, Hung, and Zheng (2003)]. The present BEM-R-[ϕ&q]-BIE and FMM-BEM solutions and exact solution have a good agreement between with ka up to 8.0.

Computation costs are compared between BEM and FMM-BEM in Fig. 3, and the relative residual v.s. iteration curve for each model is shown in Fig. 4. The figure shows that FMM-BEM is much faster, the computation cost of BEM is in the scale of $O(N^2)$, and the FMM-BEM is in the scale of $O(N)$. It can be noted that FMM-BEM is not purely $O(N)$, because the summation around the source in its neighbor

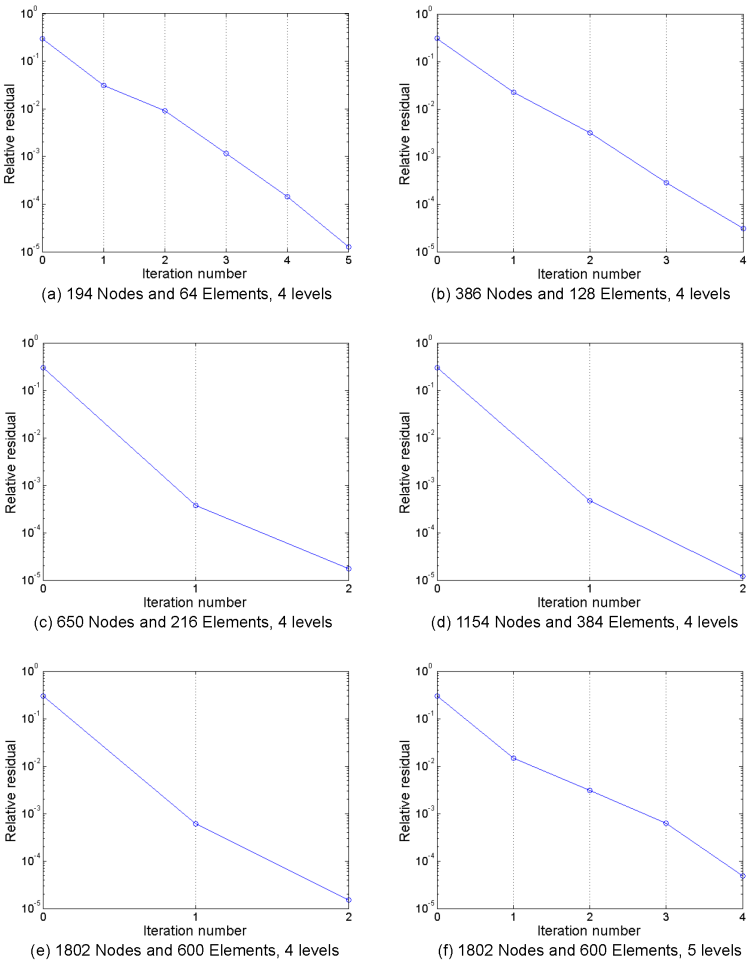

Figure 4: Comparison of iterations

clusters is done by BEM. When the node number increases, the summation in the neighbor clusters become heavy compared to far-field operation. If we control the size of leave cluster by increasing the number of levels, the computation cost will be lowered again as shown in Fig. 3.

4.2 Scattering from a UAV

To render the present method to be applicable to scattering problems, only a small change is necessary to Eq. 11, as:

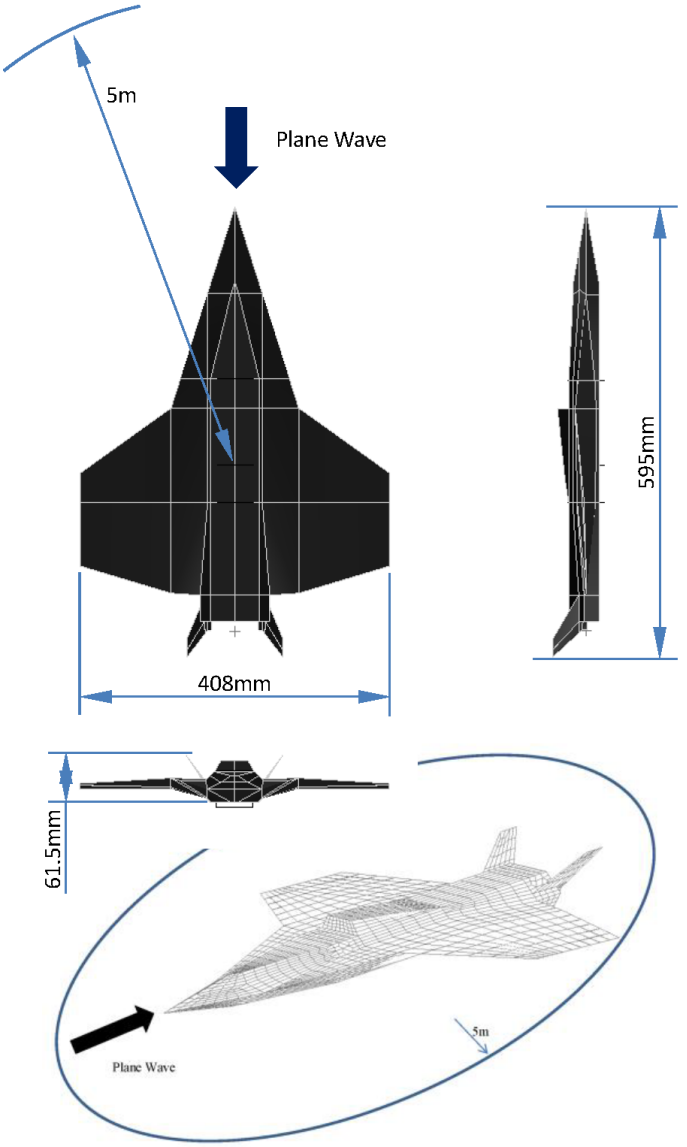

Figure 5: The geometry and the location of the UAV aircraft

$$\frac{1}{2}\phi(\mathbf{x}) - \phi^{incident}(\mathbf{x}) = \int_{\partial\Omega} q(\xi)\,\phi^*(\mathbf{x},\xi)\,dS - \int_{\partial\Omega} [\phi(\xi) - \phi(\mathbf{x})]\,\Theta^*(\mathbf{x},\xi)\,dS - \int_{\partial\Omega}^{CPV} \Theta^*(\mathbf{x},\xi)\,\phi(\mathbf{x})\,dS \tag{26}$$

where $\phi^i(\mathbf{x})$ is the incident acoustic potential; and also a similar change to Eq. 11 is needed. In this example, the acoustic scattering of plane incident waves, with a unit amplitude (e^{-ikx}), on a rigid small UAV aircraft is considered to check the practicality of the present method for large practical problems. $\partial\phi/\partial n = 0$ on the surface.

The UAV aircraft is modeled, which has a length of 595mm and width of 408mm, as shown in Figure 5. A total of 2300 Quad8 elements and 6680 nodes are used, with typical element size equal to 20mm. Velocity BCs are applied to the surface, and the model is solved at a nondimensional wavenumber $ka = 1.0$. The model was solved in 95 minutes, with the MATLAB code running on Elitebook 8560w Laptop with 4G DDR3 SDRAM memory and 2nd generation Intel Core^{TM} i7 and i5 mobile processors, with the tolerance set at 10^{-4}.

The analytical solution for the above problem is unavailable and hence the solution at the horizontal plane at $z = 0$, which is aligned with the incoming wave, is studied. The non-dimensionalized scattered pressure p_s/p_i, at distance r from the center, versus the polar angle is plotted in Figure 6.

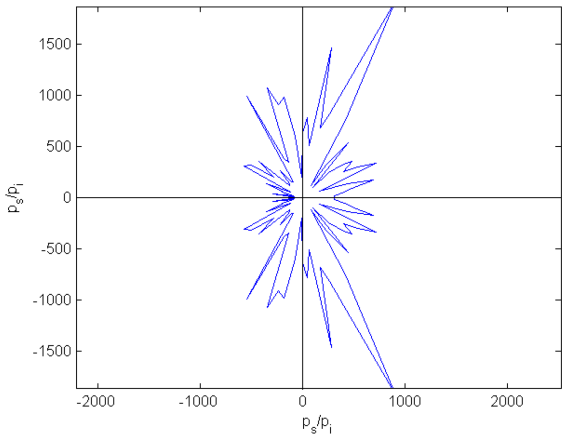

Figure 6: The angular dependence of p_s/p_i for $r = 5.0m$ and $ka = 1$

5 Closure

The weak-form of the Helmholtz differential equation, with vector test-functions (which are spatial gradients of the free-space fundamental solutions) is employed, as the basis in the present paper in order to directly derive non-hyper-singular boundary integral equations. Thereby, the difficulties with hyper-singular integrals,

involved in the composite Helmholtz integral equations presented by Burton and Miller [Burton and Miller (1971)], can be overcome. Further desingularization of the strongly singular integrals to the order of $O(r^{-1})$ is made possible with the use of certain basic identities of the fundamental solution of the Helmholtz differential equation for potential. Therefore, the formulation of the novel weakly singular $[O(r^{-1})]$ boundary integral equations is based on the weak-form of Helmholtz differential equation only. These new weakly-singular integral equations designated as R-ϕ-BIE and R-q-BIE, respectively, are solved by using direct collocations.

To speed up the numerical calculation of the boundary integral equations and overcome the drawback of fully populated system matrices in BEM further, a Chebyshev interpolation based FMM method (denoted as FMM-BEM) combined with GMRES iterative solver is utilized to implement the BEM-R-ϕ-BIE, and BEM-R-$q-$BIE. The computation cost is much lower than classical BEM, and at the scale of $O(N)$ as demonstrated by the example, which is suitable for large problems.

Acknowledgement: The work was partly supported by a collaborative research agreement with ARL and in part by DSR of the King Abdul Aziz University.

References

Alpert, B.; Beylkin, G.; Coifman, R.; Rokhlin, V. (1993): Wavelet-like bases for the fast solution of second-kind integral equations. *SIAM J. Sci. Comput.*, vol. 14, no. 1, pp. 159–184.

Brunner, D.; Junge, M.; Gaul, L. (2009): A comparison of fe-be coupling schemes for large-scale problems with fluid-structure interaction. *International Journal for Numerical Methods in Engineering*, vol. 77, no. 5, pp. 664–688.

Burton, A. J.; Miller, G. F. (1971): Application of integral equation methods to numerical solution of some exterior boundary-value problems. *Proceedings of the Royal Society of London Series a-Mathematical and Physical Sciences*, vol. 323, no. 1553, pp. 201–210.

Cheng, H.; Gimbutas, Z.; Martinsson, P. G.; Rokhlin, V. (2005): On the compression of low rank matrices. *Siam Journal on Scientific Computing*, vol. 26, no. 4, pp. 1389–1404.

Chien, C. C.; Rajiyah, H.; Atluri, S. N. (1990): An effective method for solving the hypersingular integral-equations in 3-d acoustics. *Journal of the Acoustical Society of America*, vol. 88, no. 2, pp. 918–937.

Dahmen, W.; Harbrecht, H.; Schneider, R. (2006): Compression techniques for boundary integral equations - asymptotically optimal complexity estimates. *Siam Journal on Numerical Analysis*, vol. 43, no. 6, pp. 2251–2271.

Dutt, A.; Gu, M.; Rokhlin, V. (1996): Fast algorithms for polynomial interpolation, integration, and differentiation. *Siam Journal on Numerical Analysis*, vol. 33, no. 5, pp. 1689–1711.

Dutt, A.; Rokhlin, V. (1993): Fast fourier-transforms for nonequispaced data. *Siam Journal on Scientific Computing*, vol. 14, no. 6, pp. 1368–1393.

Edelman, A.; McCorquodale, P.; Toledo, S. (1999): The future fast fourier transform? *SIAM Journal on Scientific Computing*, vol. 20, no. 3, pp. 1094–114.

Ethridge, F.; Greengard, L. (2001): A new fast-multipole accelerated poisson solver in two dimensions. *Siam Journal on Scientific Computing*, vol. 23, no. 3, pp. 741–760.

Fong, W.; Darve, E. (2009): The black-box fast multipole method. *Journal of Computational Physics*, vol. 228, no. 23, pp. 8712–8725.

Gimbutas, Z.; Greengard, L.; Minion, M. (2001): Coulomb interactions on planar structures: Inverting the square root of the laplacian. *Siam Journal on Scientific Computing*, vol. 22, no. 6, pp. 2093–2108.

Gimbutas, Z.; Rokhlin, V. (2003): A generalized fast multipole method for nonoscillatory kernels. *Siam Journal on Scientific Computing*, vol. 24, no. 3, pp. 796–817.

Greengard, L.; Rokhlin, V. (1987): A fast algorithm for particle simulations. *Journal of Computational Physics*, vol. 73, no. 2, pp. 325–348.

Han, Z. D.; Atluri, S. N. (2003): On simple formulations of weakly-singular traction & displacement bie, and their solutions through petrov-galerkin approaches. *Cmes-Computer Modeling in Engineering & Sciences*, vol. 4, no. 1, pp. 5–20.

Han, Z. D.; Atluri, S. N. (2003): Truly meshless local petrov-galerkin (mlpg) solutions of traction & displacement bies. *Cmes-Computer Modeling in Engineering & Sciences*, vol. 4, no. 6, pp. 665–678.

Liu, Y. J.; Chen, S. H. (1999): A new form of the hypersingular boundary integral equation for 3-d acoustics and its implementation with c-0 boundary elements. *Computer Methods in Applied Mechanics and Engineering*, vol. 173, no. 3-4, pp. 375–386.

Liu, Y. J.; Rizzo, F. J. (1992): A weakly singular form of the hypersingular boundary integral-equation applied to 3-d acoustic-wave problems. *Computer Methods in Applied Mechanics and Engineering*, vol. 96, no. 2, pp. 271–287.

Martinsson, P. G.; Rokhlin, V. (2007): An accelerated kernel-independent fast multipole method in one dimension. *Siam Journal on Scientific Computing*, vol. 29, no. 3, pp. 1160–1178.

Nishimura, N. (2002): Fast multipole accelerated boundary integral equation methods. *Applied Mechanics Review*, vol. 55, no. 4, pp. 299–324.

Okada, H.; Atluri, S. N. (1994): Recent developments in the field-boundary element method for finite small strain elastoplasticity. *International Journal of Solids and Structures*, vol. 31, no. 12-13, pp. 1737–1775.

Okada, H.; Rajiyah, H.; Atluri, S. N. (1988): A novel displacement gradient boundary element method for elastic stress-analysis with high-accuracy. *Journal of Applied Mechanics-Transactions of the Asme*, vol. 55, no. 4, pp. 786–794.

Okada, H.; Rajiyah, H.; Atluri, S. N. (1988): Some recent developments in finite-strain elastoplasticity using the field-boundary element method. *Computers & Structures*, vol. 30, no. 1-2, pp. 275–288.

Okada, H.; Rajiyah, H.; Atluri, S. N. (1989): Non-hyper-singular integral-representations for velocity (displacement) gradients in elastic/plastic solids. *Computational Mechanics*, vol. 4, no. 3, pp. 165–175.

Okada, H.; Rajiyah, H.; Atluri, S. N. (1990): A full tangent stiffness field-boundary-element formulation for geometric and material non-linear problems of solid mechanics. *International Journal for Numerical Methods in Engineering*, vol. 29, no. 1, pp. 15–35.

Qian, Z. Y.; Han, Z. D.; Ufimtsev, P.; Atluri, S. N. (2004): Non-hyper-singular boundary integral equations for acoustic problems, implemented by the collocation-based boundary element method. *Cmes-Computer Modeling in Engineering & Sciences*, vol. 6, no. 2, pp. 133–144.

Reut, Z. (1985): On the boundary integral methods for the exterior acoustic problem. *Journal of Sound and Vibration*, vol. 103, no. 2, pp. 297–298.

Wu, T. W.; Seybert, A. F.; Wan, G. C. (1991): On the numerical implementation of a cauchy principal value integral to insure a unique solution for acoustic radiation and scattering. *Journal of the Acoustical Society of America*, vol. 90, no. 1, pp. 554–560.

Yan, Z. Y.; Hung, K. C.; Zheng, H. (2003): Solving the hypersingular boundary integral equation in three-dimensional acoustics using a regularization relationship. *Journal of the Acoustical Society of America*, vol. 113, no. 5, pp. 2674–2683.

Ying, L. X.; Biros, G.; Zorin, D. (2004): A kernel-independent adaptive fast multipole algorithm in two and three dimensions. *Journal of Computational Physics*, vol. 196, no. 2, pp. 591–626.